Batteries & Supercaps

Review
doi.org/10.1002/batt.202400095

Chemistry Europe
European Chemical Societies Publishing

www.batteries-supercaps.org

Insights Into Electrolyte Strategies for Suppressing Side Reactions Towards Aqueous Zinc-Ion Batteries

Xuerong Gong,[a] Zongliang Zhang,[a] Zonghan Zhang,[a] Jiaxin Dai,[a] Xue Li,[a] and Baofeng Wang*[a]

Aqueous zinc-ion batteries (AZIBs) have gained significant attention as a promising technology for grid scale energy storage due to their high safety and low cost. Nevertheless, side reactions on the zinc anodes result in a decrease in effi-ciency decay and capacity loss, hindering the wide-spread application of AZIBs. Recently, great efforts have been con-ducted to tackle these challenges, such as modifying the inter-nal structure of zinc anodes, coating protection on the surface of zinc anodes, and optimizing the electrolytes. However, there is a lack of systematic summary on the design of side reac-tions-suppressed zinc anodes, especially through the optimi-zation strategies of aqueous electrolytes. Herein, this review systematically summarizes the main mechanisms and influence factors of side reactions. Subsequently, we present the main modification strategies based on electrolyte engineering for alleviating side reactions, with a particular emphasis on poly-mer electrolytes. Lastly, we shed light on the potential research directions and perspectives of aqueous electrolytes, which may promote the development of AZIBs.

1. Introduction

With the accelerated consumption of traditional energy sources and associated environment issues, the demand for secure and reliable new energy is steadily increasing.[1–4] One of the challenges associated with renewable energy sources, such as solar energy and wind energy, is their sensitivity to geographical and weather conditions. Advancing energy storage is critical to addressing these limitations. Lithium-ion batteries (LIBs) have been one of the main energy storage technologies in modern applications due to their high energy efficiency, high energy density, and long cycle life.[5–9] Although LIBs have been commercialized, the shortage of lithium resources, high costs, flammability, and low safety seriously hinder their further development.[10–14]

Recently, aqueous zinc-ion batteries (AZIBs) have become one of the most promising energy storage technologies, because of the abundance of zinc sources (75 parts per million in earth's crust), intrinsic security (non-flammable), low redox potential, high hydrogen desorption overpotential, high ion conductivity, and large theoretical capacity zinc anode.[15–18] Great progresses have been made in terms of the key component of cathode materials, aqueous electrolytes, zinc metal anodes and separators in AZIBs.[18–20]

Xianjin Gong et al.[21] achieved a dendrite-free zinc anode by introducing ZIF-8 into the $ZnSO_4$ electrolyte, which has a lifetime of 8–9 times than that of zinc anodes using the typical commercial $ZnSO_4$ electrolyte. After 500 cycles at a current density of $1\,A\,g^{-1}$, the full cell assembled using electrolyte containing ZIF-8 maintains a specific capacity of $106.1\,mAh\,g^{-1}$. Qihang Dai et al.[22] prepared the porous MnO_2 electrode using $MnSO_4$ electrolyte by the one-step electrodeposition method. Its porous structure provides more reaction sites compared to traditional electrodes. Therefore, the full cell assembled with the electrode can provide a specific area capacity of $0.35\,mAh\,cm^{-2}$ at $0.5\,mA\,cm^{-2}$. Additionally, even after 1000 cycles at a higher current density of $1.5\,mA\,cm^{-2}$, it maintains a high coulombic efficiency of 100%. However, the practical application of AZIBs is still limited by the problem of side reactions caused by active water molecules. In aqueous electrolytes, water molecules exist in two forms: free water molecules and solvated water molecules.[23] During electrodeposition, Zn^{2+} tends to form close ion pairs ($[Zn(H_2O)_6]^{2+}$) with six free water molecules, forming the solvation structure (Figure 1). The solvation effect weakens the strength of hydrogen bonding by reducing electron transfer from bonded molecular orbitals of the solvated water molecules to the unoccupied Zn^{2+} orbitals via the O–H bonding transfer of solvated Zn^{2+}.[24] During the desolvation, these solvated water molecules are more prone to participate in side reactions of hydrogen evolution reaction (HER), corrosion and the formation of by-products on the interface between the anode and electrolyte.[25] Notably, the reaction processes of HER and corrosion are influenced by the pH in the electrolyte.[26–27] In alkaline electrolytes, H_2O molecules undergo decomposition reactions during charging or discharging to generate H_2 and OH^-, which leads to an increase in the concentration of OH^- (Figure 1). Simultaneously, corrosion occurs between zinc metal and OH^-, leading to the formation of the zincate complex $Zn(OH)_4^{2-}$.[28] When the concentration of $Zn(OH)_4^{2-}$ reaches its limit of dissolution, it will dehydrate and form insoluable ZnO by-products.[29] The by-product is regarded as "dead zinc" greatly, passivates the electrode surface and increases the

[a] X. Gong, Z. Zhang, Z. Zhang, J. Dai, X. Li, Dr. B. Wang
Shanghai Key Laboratory of Materials Protection and Advanced Materials in Electric Power
Shanghai University of Electric Power
201306 Shanghai, China
E-mail: wangbaofeng@shiep.edu.cn

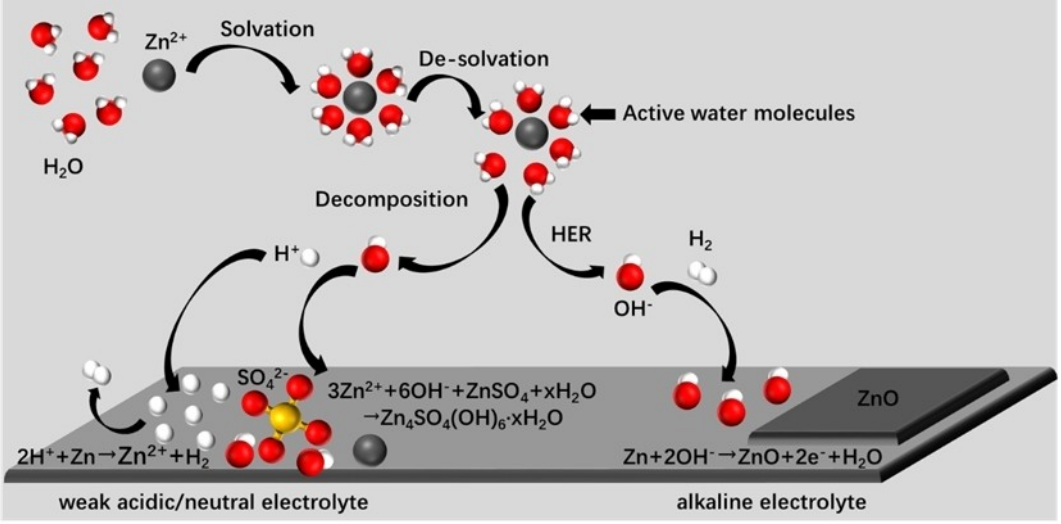

Figure 1. Schematic illustration of Zn^{2+} solvation process and side reactions between zinc metal anode and different electrolytes.

internal resistance, leads to the unreversibility and capacity fading of the zinc anode.[14] The corresponding reaction equations are

$$2H_2O + 2e^- \rightarrow H_2 \uparrow + 2OH^- \quad (1),$$

$$Zn + 4OH^- \leftrightarrow Zn(OH)_4^{2-} + 2e^- \quad (2)$$

$$\text{and } Zn(OH)_4^{2-} \leftrightarrow ZnO + H_2O + 2OH^- \quad (3).$$

In weakly acidic or neutral electrolytes, when a single zinc anode reacts with the electrolyte, many microcells are formed, leading to the escape of H_2 and an increase in OH^- concentration (Figure 1). The increase in OH^- concentration makes it easier to form $Zn_4SO_4(OH)_6 \cdot xH_2O$ by-product.[30–33] Notably, despite $Zn_4SO_4(OH)_6 \cdot xH_2O$ is generated on the Zn/electrolyte interface, its loose and porous structure cannot prevent the electrolytes from reaching the surface of the Zn anode to suppress side reactions.[29,34] Thus, the zinc metal reacts continuously with the electrolyte on the interface until one of them runs out completely, which results in a low coulombic efficiency (CE) and unstable cycling performance of batteries.[18,25] The corresponding reaction equations are

$$2H^+ + Zn \rightarrow Zn^{2+} + H_2 \uparrow \quad (4),$$

$$\text{and } 3Zn^{2+} + 6OH^- + ZnSO_4 + xH_2O \rightarrow Zn_4SO_4(OH)_6 \cdot xH_2O \quad (5),$$

respectively. Therefore, it is urgent to solve the problem of side reactions existing in the anode, and achieve long life and high performance AZIBs.

Up to now, numerous strategies have been proposed to alleviate side reactions, such as modifying the internal structure of zinc anodes,[35–37] coating protection on the surface of zinc anodes,[38–40] and optimizing the electrolytes.[41–44] Among these, electrolyte engineering can not only solve the problems of side reactions and zinc dendrites on zinc anodes, but also solve the problems of poor stability of the cathode materials and narrow electrochemical window caused by electrolytes.[45–47]

In this review, potential electrolyte optimization strategies to suppress side reactions, will be discussed. Based on the structural characteristics of electrolytes, these strategies are summarized from two aspects of liquid and polymer. Moreover, the functions of specific strategies, such as occupying the sites of active water molecules on the zinc anode and modifying the solvation structure of Zn^{2+} by substituting activity water molecules or inhibiting activity water molecules, are analyzed in detail. Lastly, the further development of the optimization strategies for aqueous electrolytes is prospected, which will provide additional guidance for researchers in this field.

Xuerong Gong is currently pursuing the master's degree at Shanghai University of Electric Power. Her current research focuses on aqueous zinc-ion batteries.

Baofeng Wang is a Full Professor at Shanghai University of Electric Power, China. His Ph.D. (2004) was obtained from the Shanghai Institute of Microsystem and Information Technology, CAS. He then worked as a lecturer at Shanghai Jiao Tong University and visiting research fellow at University of Wollongong and Fudan University. His research interests focus on the key materials (cathode and anode materials, electrolytes, binders) for new chemical power sources.

2. Optimization Strategies for Aqueous Liquid Electrolytes

Traditional liquid electrolytes suffer from various challenges, including HER, corrosion, and the formation of by-products. To solve the above problems, various effective strategies have been dedicated to regulate the solvation structure of Zn^{2+} or prevent water molecules from participating in interfacial reactions. In this section, these strategies are divided into three main categories, including the optimization of anionic salts, the application of additives and the regulation of electrolyte concentration.

2.1. Optimization of Anionic Salts

The coordination ability of anions with Zn^{2+} is influenced by several factors, including ion radius and charge density and solubility.[48–52] Anions with great water solubility are more likely to form coordination compounds with Zn^{2+} in an aqueous solution.[48–49] Anions with smaller ionic radius and higher charge density tend to establish stronger metal-oxygen coordination bonds, thereby enhancing their ability to coordinate with Zn^{2+}.[50–52] Anions possessing the strong coordination ability with Zn^{2+}, can replace active water molecules in typical solvation structures, altering the solvation structure of Zn^{2+}. Currently, researches on anionic salts have mainly focused on $ZnSO_4$, $Zn(ClO_4)_2$, $Zn(CH_3COO)_2$, $Zn(CF_3SO_3)_2$, and $Zn(TFSI)_2$ electrolytes.[50,53–57] As shown in Figure 2a, the application of $ZnSO_4$ and $Zn(CH_3COO)_2$ electrolytes produces $Zn_4SO_4(OH)_6 \cdot xH_2O$ and carboxyl-containing by-products, respectively. In contrast, ClO_4^- creates a thin layer on the surface of Zn, which provides a potential gradient across the layer and allows Zn deposition underneath it. The mechanism is similar to the protective layer formed by LiCl on top of lithium in LIBs. Therefore, the uniform coverage of ClO_4^- on the zinc surface effectively suppresses the interaction between zinc and electrolyte, hindering the formation of by-products. Compared with $ZnSO_4$ electrolyte, $Zn(CF_3SO_3)_2$ electrolyte exhibit higher response current and smaller potential separation during Zn electroplating/stripping (Figure 2b). This indicats that $Zn(CF_3SO_3)_2$ electrolyte have faster kinetics of Zn deposition/dissolution. The voltammetry in $Zn(CF_3SO_3)_2$ electrolyte further proves the reversibility of Zn deposition/dissolution (Figure 2c). Chaohua Sun et al.[58] investigated the impact of $CF_3SO_3^-$ on the solvation shell of Zn^{2+}. Molecular dynamics (MD) simulations show that $CF_3SO_3^-$ can replace some active water molecules around Zn^{2+}, altering the solvation structure (Figure 2d). Radial distribution functions (RDFs) for $Zn(CF_3SO_3)_2$ electrolyte show that the Zn–O peaks originated from H_2O and $CF_3SO_3^-$ both appear ~2 Å from Zn^{2+}, indicating that $CF_3SO_3^-$ enter the solvated shell (Figure 2e and f). As a result, the transport and charge transfer of Zn^{2+} are improved by the decrease in the number of active water molecules surrounding it. Tzu-Ho Wu et al.[60] demonstrate the effects of 2 mol (M) $Zn(TFSI)_2$ electrolyte on reversibility of zinc anode. Ex situ X-ray diffraction patterns of cathodes in $Zn(TFSI)_2$ electrolyte show that there is no obvious by-product signal during the entire charging and discharging process. This proves that $Zn(TFSI)_2$ electrolyte have the ability to regulate the solvation structure because of the presence of $CF_3SO_3^-$. In addition, $Zn(TFSI)_2$ have a wide electrochemical window (3.32 V vs. Zn/Zn^{2+}), and good compatibility with metallic Zn.[27,59–60] While these anionic salts can effectively improve the CE and cycling stability of batteries, their high cost makes it challenging to achieve commercial viability.

2.2. Application of Additives

Electrolyte additives are widely used to improve the performance of batteries.[61–62] In AZIBs, organic solvent additives and

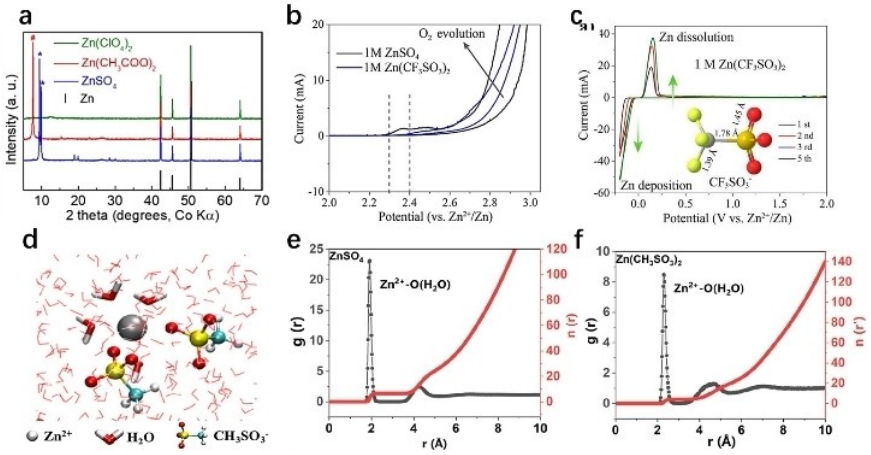

Figure 2. (a) X-ray diffraction (XRD) patterns of Zn anodes in 1 M $ZnSO_4$, $Zn(CH_3COO)_2$, and $Zn(ClO_4)_2$ electrolytes after 50 cycles.[50] (b) Electrochemical stability for 1 M $ZnSO_4$ and 1 M $Zn(CF_3SO_3)_2$ electrolyte, respectively.[46] (c) Cyclic voltammograms (CV) of Zn electrode in aqueous electrolyte of 1 M $Zn(CF_3SO_3)_2$ at the scan rate of 0.5 mV s^{-1} between −0.2 and 2.0 V.[46] (d) Three-dimensional snapshot of the $Zn(CH_3SO_3)_2$ system obtained from MD simulations and a partially enlarged snapshot representing the Zn^{2+} solvation structure. RDFs for Zn^{2+}–O (H_2O) collected from MD simulations in (e) $ZnSO_4$ and (f) $Zn(CH_3SO_3)_2$. D–F reproduced with permission.[58]

zinc-philic additives are used to improve the reversibility of zinc anodes.[17,63–64]

Compared to H_2O, organic solvent additives have the stronger coordination ability, which substitutes active water molecules to modify the solvation structure of Zn^{2+}, thus improving the desolvation and deposition processes during electrochemical reactions in AZIBs.[65–66] A large amount of organic solvent additives, such as methanol,[67] N,N-dimethylacetamide (DMA),[63] and ethylenediamine tetraacetic acid (EDTA),[68–70] have been used to excludes H_2O from the Zn^{2+} solvation sheath. A cost-effective and green glycine (Gly) additive is applied to stabilize the Zn anode.[71] DFT calculations show that the binding energies (BE) value of $[Zn(H_2O)_6]^{2+}$ is lower than that of the $[Zn(H_2O)_5(Gly)]^{2+}$ and $[Zn(H_2O)_4(Gly^-)]^+$ (Figure 3a). This confirms that when Gly molecule or anion replaces water molecules in $[Zn(H_2O)_6]^{2+}$, they coordinate with Zn^{2+} to form the more stable chemical bond. This stronger coordination bond weakens the electrostatic repulsion between neighboring Zn^{2+} species, which can be demonstrated by electrostatic potential (ESP) mapping (Figure 3b). Wu et al.[63] reported a high donor number N, N-dimethylacetamide (DMA) additive. Compared with water molecules, DMA molecules have a higher gutmann donor number (DN) and abundant polar groups. As a result, it can form H-bonds to trap free water molecules, inhibiting HER on the zinc anode by weakening the activity of water molecules (Figure 3c and d). Furthermore, MD simulations show that DMA can modulate the solvation structure of Zn^{2+} (Figure 3e). The addition of DMA results in a significant reduction of the peak corresponding to SO_4^{2-} stretching vibration in the fourier transform infrared spectroscopy (FTIR) spectra (Figure 3f). This proves the formation of coordination interaction between DMA and Zn^{2+}, which regulates the coordination environment of Zn^{2+}. Therefore, Zn//Zn batteries assembled from electrolyte systems containing 10 vol% DMA and zinc sulfate have highly reversible zinc plating/stripping performance, which can achieve an exceptionally long cycle life of 1900 hours at 1.0 mA cm^{-2} and 1.0 mAh cm^{-2}, approximately four times that of batteries using $ZnSO_4$ electrolytes. In addition, inorganic polar oxides with hydroxyl groups on the surface, including SiO_2, TiO_2, and Al_2O_3, can interact with water molecules and influence the solvation structure of Zn^{2+}.[72] Rongyu Deng et al.[72] developed an aqueous 'soggy-sand' electrolyte by evenly dispersing Al_2O_3 particles into a typical $ZnSO_4$ solution. Al_2O_3 exhibits inherent capabilities to adsorb ions and H_2O molecules. Initially, H_2O molecules are physically adsorbed onto Al_2O_3 particles. Subsequently, more H_2O molecules and SO_4^{2-} ions undergo chemical adsorption through hydrogen bonding near the hydroxyl groups. The adsorption of H_2O molecules diminishes the activity of water, mitigates side reactions, and widens the electrochemical window. Consequently, in the battery systems with the 'soggy-sand' electrolyte, Zn//Zn batteries demonstrate an extended lifespan and dendrite-free deposition for up to 2500 hours, and Zn/MnO_2 full battery exhibits a high charging cutoff voltage of 2 V (relative to Zn^{2+}/Zn) and a specific capacity of 344 mAh g^{-1} at a current density of 1 A g^{-1}.

Unlike organic solvent additives, zinc-philic additives mainly exert their effects by adsorbing on the surface of the zinc anode. DFT calculations of adsorption energy indicate that the binding energy between zinc-philic additives, including Rb_2SO_4, sorbitol and Gly, and zinc anodes is stronger than that of water molecules (Figure 4a). This strong interaction enables these additives to adsorb on the zinc anode surface and occupy the active sites of water molecules, forming a poor-H_2O layer. This surface passivation strategy can prevent active water molecules from reaching the surface of the zinc anode and participating in side reactions.[24,73] Cong Huang et al.[74] employed saccharin (Sac) to regulate the electrical double layer (EDL) structure on the zinc anode/electrolyte interface (AEI). The decrease in peak density of C=O and the appearance of a new N–Zn bond characteristic peak in the high-resolution X-ray Photoelectron Spectroscopy (XPS) spectra confirm the interaction between Sac

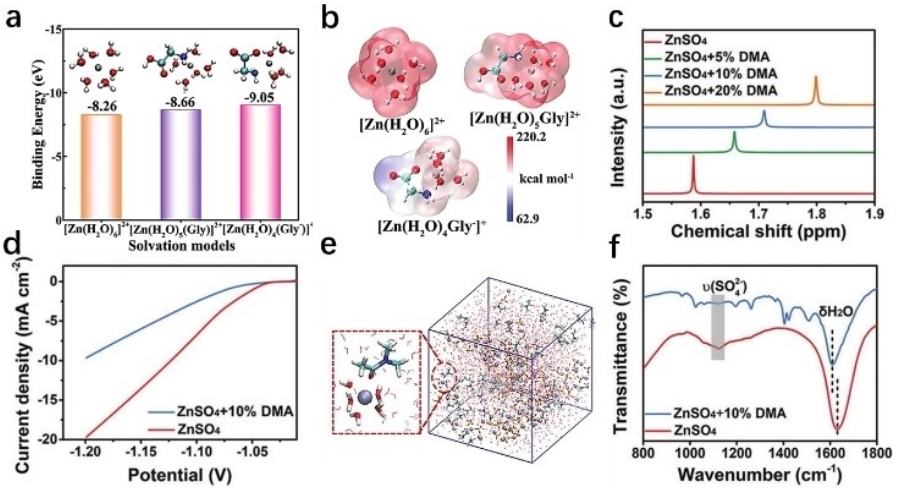

Figure 3. (a) DFT calculation of the binding energies and (b) ESP mapping for original $[Zn(H_2O)_6]^{2+}$, $[Zn(H_2O)_5(Gly)]^{2+}$, and $[Zn(H_2O)_4(Gly)]^+$ hybrid cluster.[71] (c) 1H Nuclear Magnetic Resonance (NMR) spectra of H2O in ZnSO4 solutions containing 0%, 5%, 10%, 20% DMA. (d) Linear Sweep Voltammetry (LSV) curves of Zn anodes in $ZnSO_4$ and $ZnSO_4$ + 10% DMA electrolytes. (e) Snapshot of $ZnSO_4$ + DMA electrolyte system obtained from MD simulation. (f) FTIR spectra of $ZnSO_4$ and $ZnSO_4$ + 10% DMA electrolytes. C–F reproduced with permission.[63]

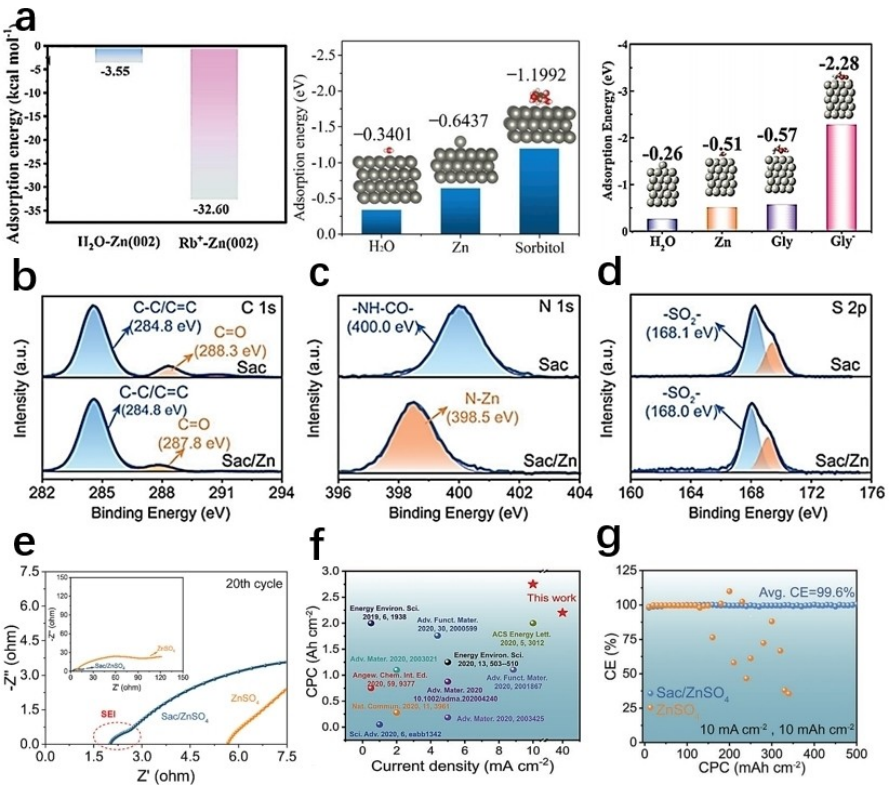

Figure 4. (a) The adsorption energy of different molecules/ions onto Zn (002) surface.[71,75–76] The High-resolution XPS spectra of Sac and Sac/Zn: (b) C 1s; (c) N 1s; (d) S 2p. (e) The Electrochemical Impedance Spectroscopy (EIS) results of Zn symmetric cells cycled in $ZnSO_4$ and Sac/$ZnSO_4$ electrolyte. (f) The CPC comparison of Zn symmetric cell using Sac/$ZnSO_4$ electrolyte with other reported literatures. (g) The CE of Zn|Cu half cells using Sac/$ZnSO_4$ and $ZnSO_4$ electrolyte. B–G Reproduced with permission.[74]

and Zn metal (Figure 4b–d). This interaction leads to the emergence of a novel type of EDL structure with water deficiency. A specialized solid electrolyte interface (SEI) is established on the surface of the zinc anode as a result of the decomposition of Sac anions (Figure 4e), mitigating side reactions and regulating zinc deposition. The Sac electrolyte system can increase the cumulative plating capacity (CPC) of Zn//Zn batteries (10 mA cm^{-2}, 10 mAh cm^{-2}) by 2.75 Ah cm^{-2}, and the average CE of Cu//Zn batteries is 99.6% (Figure 4f and g). Additives can also introduce some challenges. The adsorption of additives can increase the energy barrier for Zn^{2+} desolvation, causing slower diffusion kinetics of Zn^{2+}. Over-absorption of additives on the zinc anode may increase electrode polarization, reducing ion conductivity.

2.3. Regulation of Eectrolyte Concentration

It is effective to adjust the salt concentration of the electrolyte to improve the CE of zinc plating.[77–79] Increasing the salt concentration of the electrolyte can effectively suppress side reactions.[78–79] On one hand, increasing salt concentration in the electrolyte and decreasing water concentration in the electrolyte will result in a decrease of the equilibrium potential of H_2O/H_2. This directly reduces the escape of H_2.[80] On the other hand, as the salt concentration increases, electrolyte will form strong electrostatic interactions with water molecules. This interaction will weaken the hydrogen bonds of water molecules, thereby inhibiting their activity.[81–82] In recent years, significant interest has been seen in the development and study of high concentration electrolytes.[83] the expensive cost of high concentration electrolytes poses challenges to its commercial feasibility. To lower the cost of electrolytes, some high concentrations of cationic salts are introduced into the electrolyte containing zinc salts, because the regulation of the solvation structure mainly through anions entering the solvation shell. Y. Zhu et al.[84] designed a Zn^{2+}-based electrolyte using high concentration of sodium salt (0.5 m $Zn(ClO_4)_2$ and 18 m $NaClO_4$). The ^{17}O (water) NMR spectra of different electrolytes indicates that as the concentration of $NaClO_4$ electrolyte increases, the hydrogen bonds between water molecules are disrupted (Figure 5a), and the activity of water molecules is inhibited, effectively weakening the H_2O-induced side reactions. The concentration of electrolytes further increases until the hydrogen bonds between water molecules are completely disrupted, which causes water molecules to be surrounded by electrolyte ions and then to form a hydration layer with these ions. On this basis, the concept of "water in salt" is proposed.[57,85–86] Compared to $ZnSO_4$ electrolyte, $ZnCl_2$ electrolyte has a higher solubility in water, which is beneficial to form a higher concentration electrolyte.[82,87] Wang et al.[87] used a 30 M $ZnCl_2$ electrolyte in a Zn/MoO_3 cell. The high concen-

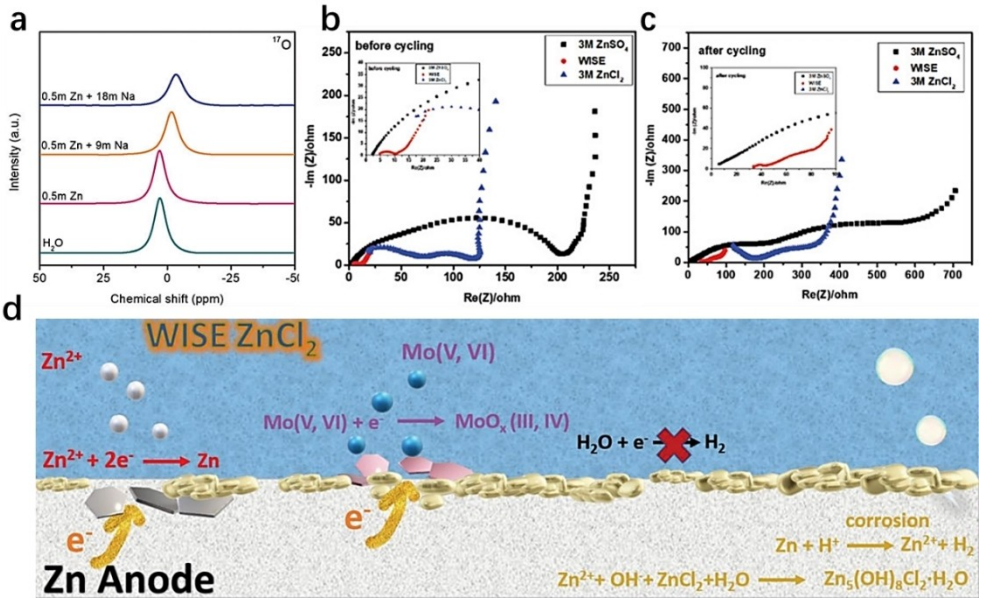

Figure 5. (a) ^{17}O (water) NMR spectra of different electrolytes.[84] EIS Nyquist plots of cells (b) before and (c) after rate capability test in three electrolytes. (d) Schematic showing the plausible reaction mechanisms at Zn anode in 30 m $ZnCl_2$ WISE. B–D are reproduced with permission.[87]

tration of $ZnCl_2$ electrolyte not only reduces the interfacial charge transfer impedance (Figure 5b and c), but also forms a unique highly crystalline $Zn_5(OH)_8Cl_2$–H_2O solvation structure (Figure 5d). The electrochemical stability window is broadened by increasing the overpotentials of HER and oxygen evolution reaction (OER). The cell assembled with 30 M $ZnCl_2$ electrolyte has excellent cycle capacity and long cycle life. A capacity retention of 73% can be achieved after 100 cycles at 100 mA g^{-1}, and no significant capacity degradation is observed at high current densities of 2 A g^{-1}. However, batteries assembled with high concentration electrolytes are more likely to occur high voltage polarization in low current density situations. Therefore, there is a tendency to develop electrolytes with intermediate concentrations or localized "salt-in-water" structures to reduce the cost.[40,88]

3. Optimization Strategies for Aqueous Polymer Electrolytes

Unlike liquid electrolytes, aqueous polymer electrolytes have a special network structure.[89–92]

Typical polymer electrolytes prepared with polyacrylamide (PAM)[46,93–95] and polyacrylic acid (PAA)[96–97] formed a chemical cross-linking network through covalent bonds, which brings high mechanical strength and water-retention performance. The network structure reduces the content and activity of water molecules in the electrolyte, which is beneficial for suppressing side reactions.[89–91] Meanwhile, the network structure with mechanical properties suppresses the growth of zinc dendrites, indirectly alleviating side effects.[91–92] However, once covalent bonds break, it is difficult to recover the original network structure. This results in a decrease in the mechanical strength and integrity of the network structure. Meanwhile, the water retention capacity of single network structures is limited, which makes it difficult to completely inhibit water molecules' activity. To inhibit side effects, two strategies are proposed, including modification of the network structure and the electrolyte in the network structure.

3.1. Modification of the Network Structure

At present, various strategies for modifying the network structure of polymer electrolytes mainly focus on forming the multi-crosslinked network structure.[98–103] To build multi-crosslinked network structure, a wide range of materials, including polymer materials, ionic compounds, and inorganic materials, have been introduced into aforementioned typical polymer electrolytes with a single network structure.

Polymer materials, including guar gum (GG),[30,104] cellulose[14,98,105–106] and sodium alginate,[107–108] possess abundant hydrophilic groups. These hydrophilic groups on polymer materials react with the functional groups within synthetic polymers to form reversible non-covalent bonds, such as hydrogen bonding and intermolecular forces. Materials construct a multi-crosslinked network structure through these reversible non covalent bonds.[30,46,94] With the addition of polymer materials, there is an increase in the amount of bound water in the multi-crosslinked network, which caused by the strong attraction between hydrophilic groups and water molecules. This directly reduces the amount of free water molecules on the zinc/electrolyte interface, thereby weakening HER. In addition, the increase in bound water molecules disrupts the hydrogen bonds between free water molecules, which leads to a reduction of active water molecules, suppressing the H_2O-induced side reactions.[91,109] Wang et al.[93] synthe-

sized a ternary cross-linked polymer electrolyte (PCS) comprising PAM, carboxymethyl cellulose, and starch. The presence of starch, which is abundant in hydroxyl groups, contributes to the hydrophilic network structure of PCS. When $ZnSO_4$ dissolves in water, due to the low energy barrier of Zn^{2+}, a large amount of Zn_{2+} is connected to six water molecules in the form of $[Zn^{2+}(H_2O)_6SO_4^{2-}]$ (solvent separated ion pair SIPs). In the Raman spectra of different electrolytes (Figure 6a), the intensity change of SIPs indicates that PCS can inhibit the formation of solvated structures $[Zn(H_2O)_6]^{2+}$. In the FTIR spectra of different electrolytes (Figure 6b), the gradual weakening of the stretching and bending vibration for the H–O bending (water) proves that with the introduction of starch, the hydrogen bonds between water molecules are broken, and the activity of water molecules is weakened. In XRD patterns of the zinc anode in PCS (Figure 6c), there is no obvious by-products signal, indicating that PCS effectively inhibits the occurrence of by-products on the Zn anode. These results demonstrate that hydroxyl groups on PCS inhibit the activity of water molecules through hydrogen bonding, thereby regulating the solvation shell of Zn^{2+} and effectively preventing active water molecules from participating in side reactions. Additionally, the carboxylic groups present in the PCS network structure can promote uniform Zn deposition while hindering the formation of zinc dendrites. When using PCS electrolyte, the Zn//Zn symmetric battery can cycle up to 4900 hours while the Zn//MnO_2 battery can cycle up to 1000 times under 1 A g^{-1} conditions, with a CE of up to 99.5 %. The introduction of hydrophilic polymer materials can enhance the network structure of the polymer electrolyte by forming physical cross-linking network through hydrogen bonding.[98,110] However, it is worth noting that the variations in main chain structures and the quantity and types of polar groups among different hydrophilic materials result in different hydrogen bonding networks in polymer electrolytes.[94,111–113] These variations can significantly impact the performance of the polymer electrolyte, including its mechanical properties, water retention ability and low-temperature performance.[94,114] Caoer Jia et al.[94] designed a ternary cross-linked polymer electrolyte (PCG) comprising PAM, CMC, and CG. A large number of hydroxyl groups on the CG chain form hydrogen bonds with PAM and CMC, forming a physical crosslinking network (Figure 6d and e). The network structure with uniform and compact small pores improves water retention, mechanical properties and low temperature properties of PCG electrolyte. CG transforms considerable free water into bound water through hydrogen bonding, elevating bound water content and rendering water molecules in the gel less prone to evaporation (Figure 6f). The hydrophilic network structure reduces the freezing point of PCG electrolyte to −48 °C, enhances its tensile performance, and maintains relative stability at −20 °C. (Figure 6g–i). Therefore,

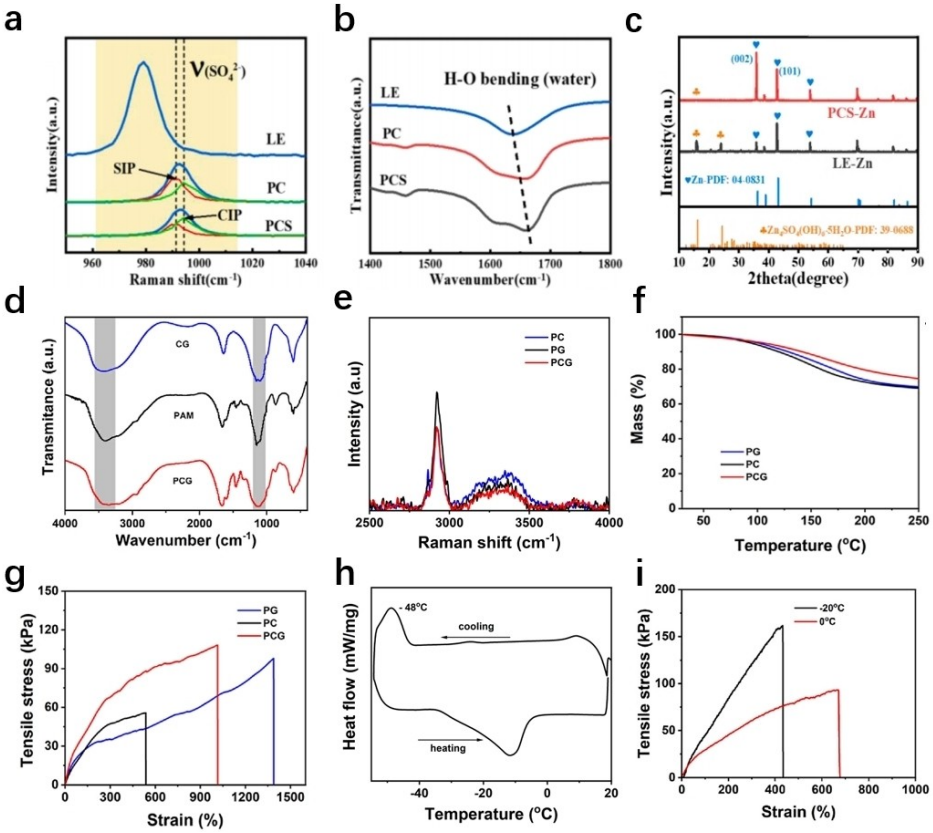

Figure 6. (a) Characteristic peaks of SO_4^{2-} in Raman spectra of different electrolytes. (b) FTIR spectra of different electrolytes. (c) XRD images of Zn electrodes after 100 charge-discharge cycles in liquid and PCS electrolytes. A–C are reproduced with permission.[93] (d) FT-IR spectra of PAM, CG, and PCG. (e) Raman spectra. (f) TGA curves. and (g) Stress-strain curves of the PC, PG, and PCG electrolytes. (h) DSC curves of the PCG electrolyte. (i) Stress-strain curves of PCG electrolyte at −20 °C and 0 °C. D–I are reproduced with permission.[94]

Zn//Zn batteries assembled with PCG can maintain a stable zinc plating/stripping process for over 1100 hours. Full batteries assembled with PCG can maintain a high capacity retention rate of 108.3% after 100 cycles at −20 °C and a current density of 1 $A g^{-1}$, and deliver a reversible capacity of 51.6 $mAh g^{-1}$ after 10000 cycles at 0 °C and a current density of 10 $A g^{-1}$, with a capacity retention rate of 72.7%. Unfortunately, despite the differences in hydrogen bonding networks constructed by different hydrophilic materials, researchers have not conducted in-depth and systematic investigations into the reasons for these differences.

In addition to the introduction of polymer materials with polar groups in its main chain, the utilization of ionic compounds can also construct new network structures. Ionic compounds, including cations (Zn^{2+}, Fe^{3+} and so on[99–100,115]) and anions (ClO_4^-, Cl^- and so on[116–119]), react with functional groups on synthetic polymer materials to form reversible non-covalent bonds, such as ionic and hydrogen bonds, preparing polymer electrolytes with chemical cross-linking network structure and physical cross-linking network structure. The physical cross-linking network structure of polymer electrolytes dissipate energy through the breaking of non-covalent bonds.[99] This property gives polymer electrolytes self-healing ability and improves their toughness. Yan Huang et al.[99] polymerized acrylic acid (AA) monomer with ferric chloride ($FeCl_3$) to form Fe^{3+}-crosslinked PANa hydrogel ($PANaFe^{3+}$). Ionic bonds formed between Fe^{3+} and the PANa chains can be reconnected, which brings self-healing ability and good flexibility of $PANaFe^{3+}$. After undergoing self-healing, the $PANaFe^{3+}$ hydrogel retains its exceptional mechanical properties, with a tensile strain of approximately 1000% (Figure 7a). Huang et al.[118] developed a polysaccharide polymer electrolyte (CSAM-C) with a high ductility and a low concentration of $Zn(ClO_4)_2$. A ternary cross-linked structure is formed by water, polymer chains, and ClO_4^-, which enhances the mechanical strength of polymer electrolytes (Figure 7b–e). The area ratio of the strong, medium, and weak hydrogen bond (HB) for water in different hydropolymer electrolytes are fitted by gaussian curve fitting (Figure 7f). These results reveal a substantial increase in the content of weak hydrogen bonds in CSAM–C, accompanied by a significant decrease in the content of strong hydrogen bonds. In the NMR spectra of water molecules in $Zn(ClO_4)_2$ and $ZnSO_4$ solution (Figure 7g and h), unlike $ZnSO_4$ electrolyte, as the concentration of $Zn(ClO_4)_2$ increases, the 1H peak shifts to a lower field, indicating that the hydrogen bonds of water molecules are weakened due to the presence of ClO_4^-. This is because the hofmeister effect enables ClO_4^- to form feeble hydrogen bonds with water molecules in polymer electrolytes, disrupting the hydrogen bonds between water molecules and limiting the content and activity of water molecules. Consequently, the freezing point of water is effectively reduced by CSAM–C. When CSAM–C is used to build a battery, the symmetrical zinc battery displays no apparent dendrites after Zn plating/stripping for more than 1200 hours. However, in

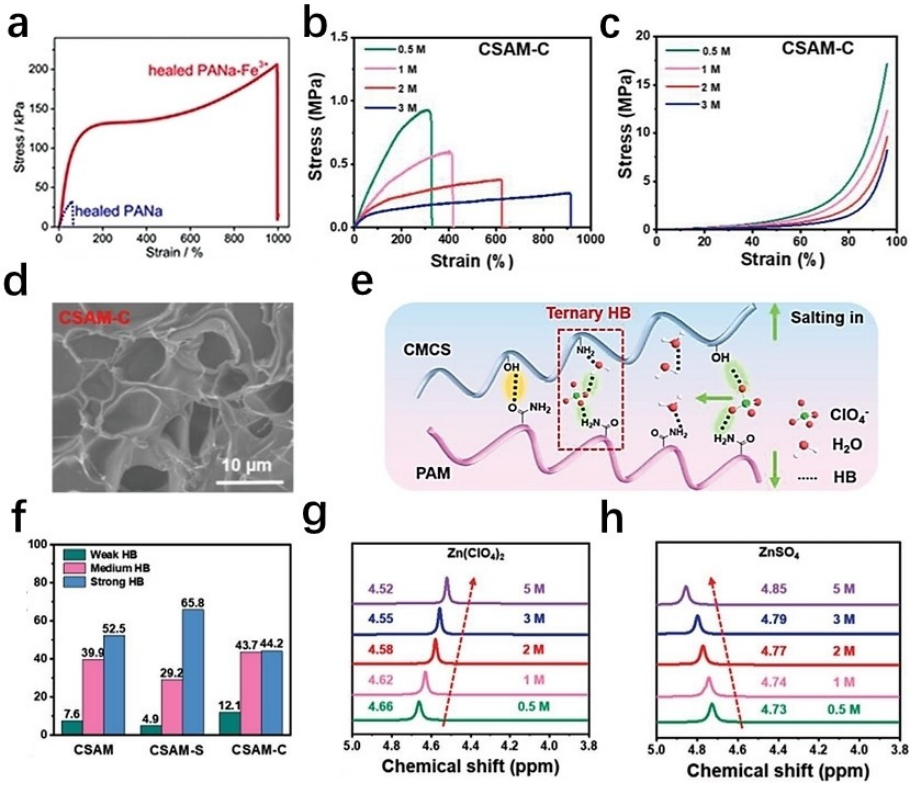

Figure 7. (a) Stress-strain curves of $PANaFe^{3+}$ vs. PANa hydrogel.[99] (b) Tensile and (c) compressive stress-strain curves of the CSAM–C hydropolymer immersed in $Zn(ClO_4)_2$ solutions of different concentrations. (d) SEM images of CSAM–C hydropolymers. (e) Schematic diagram of the interactions among CMCS, ClO_4^-, and PAM chains in CSAM–C hydropolymer. (f) Summary of the area ratio of the strong, medium, and weak HB for water in different hydropolymer electrolytes. ^1H NMR spectra of water molecules in (g) $Zn(ClO_4)_2$ solution and (h) $ZnSO_4$ solution with different concentrations. B–H Reproduced with permission.[118]

some cases, the migration and deposition of halogen ions on the electrode surface within the electrolyte may occur. This phenomenon will result in electrode polarization, ultimately leading to a decline in battery performance.

Besides the utilization of ionic compounds, the incorporation of inorganic materials has also been implemented to enhance the mechanical properties of the network structure. Inorganic materials, including carbon nanotubes (CNTs),[95,120–121] graphene,[101–103] nano-ZrO_2[122] and ceramic filler,[123] have good conductivity and high mechanical properties. Researchers modified inorganic materials by grafting hydrophilic groups, allowing them to interact with functional groups on synthetic polymer materials to improve the mechanical properties of polymer electrolytes.[101–102] In order to increase the solubility of carbon nanotubes in aqueous solution, Emine S et al.[121] prepared functionalized carbon nanotubes (fCNTs) by increasing the number of hydrophilic carboxyl (−COOH) groups on the carbon nanotubes through microwave treatment. The fCNTs doped gel electrolyte system (fCNTGE) is prepared by adding fCNTs into PVA-based gel electrolyte. DFT calculations indicate that as the number of −COOH groups increases, the interaction between PVA chains and fCNTs becomes stronger, further improving the mechanical properties. Therefore, fCNTGE has a tensile strength (22.3 kPa), 2.5 times that of typical gel electrolyte (GE). Haoyu Mi et al.[101] introduced graphene oxide (GO) into SA and PAM dual networks to prepare composite gel electrolyte (SAG). SAG has an ion conductivity of 12.12 mS cm^{-1} due to the introduction of GO with good conductivity (Figure 8a). In addition, the stress-strain curve and deformation diagram demonstrate that SAG has high mechanical strength (Figure 8b and c). After 500 charges and discharges at 1 C, the discharge specific capacity retention rate of the Zn/SAG/$LiFePO_4$ battery assembled by SAG is 63.3 %, and the CE is about 100 %. However, the preparation cost of nano- materials is relatively high, which may increase the production cost of zinc-ion batteries. This may affect the commercial application of nanomaterials.

3.2. Modification of Electrolytes in the Network Structure

The optimization of polymer electrolytes can also be achieved by modifying the electrolyte in the network structure. The application of electrolyte additives can improve the ion conductivity, electrode stability, and thermal stability of polymer electrolytes.[124–128]. Pengfei Zhou et.al[129] achieved $Na_{1+x}Zr_2Si_xP_{3-x}O_{12}$ (NASICONs) polymer electrolyte with fewer defects by incorporating MgF_2 additive. The total room-temperature ionic conductivity of NASICONs with 1 1wt% MgF_2 can reach 2.03 mS cm^{-1}, which is about 181.3 % higher than the electrolyte without MgF_2. Kanghyeon Kim et.al[130] used 2-(Trimethylsilyl)ethanethiol (TMS-SH) as an polymer electrolyte additive. TMS-SH is oxidized and decomposed during the charging process, forming a stable solid electrolyte interphase (CEI). The CEI inhibits interface degradation between the cathode and the polymer electrolyte, thereby improving the stability of the cathode interface. Isala Dueramae et al[131] prepared a carboxymethyl cellulose (CMC)/poly (N-isopropylacrylamide) (PNiPAM) polymer electrolyte. The thermal degradation of CMC was inhibited by introducing the additive PNiPAM, improving the thermal stability of the battery. However, the application of additives in polymer electrolytes is challenging due to the complex preparation process for photopolymerization or thermal polymerization. Additives need to possess thermal or optical stability to withstand the polymerization conditions, ensuring that they will not be degraded during the preparation process. In addition, additives should exhibit flexibility in migration within the network structure, which allows them to distribute evenly. Therefore, additives that adsorb on the surface of zinc anodes to exert their effects are unsuitable for application due to the limitations of the network structure of polymer electrolytes. To relieve side reactions, organic solvent additives, such as dimethyl sulfoxide (DMSO)[30,132] and glycerol,[133–134] which inhibit the activity of water molecules by breaking hydrogen bonds between water molecules, are introduced into polymer electrolytes. Researchers Liu et al.[132] devised a functional double network hydropolymer electrolyte (FDHE) using dimethyl sulfoxide (DMSO) as the H receptor and solvation regulator during synthesis (Figure 9a). The hydrogen bond strength of H_2O–H_2O (~19 KJ mol^{-1}) and H_2O–DMSO (~22 KJ mol^{-1}) are calculated by DFT calculations (Figure 9b). This indicates that DMSO, as the H receptor, forms stronger hydrogen bonds with free water molecules, significantly altering the original hydrogen bond structure of water molecules. The destruction of hydrogen bonding structure reduces the activity of water and inhibits the crystallization of electrolyte, inhibiting HER and improving the low-temperature performance of batteries. DFT calculations show that the

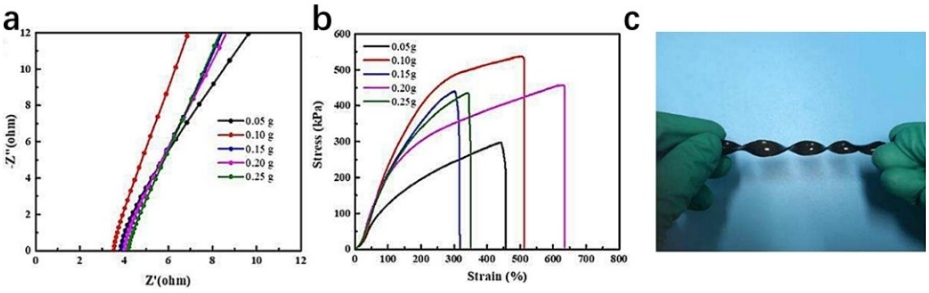

Figure 8. (a) the ionic conductivity of SAG with different amount of GO. (b) Stress–strain curves of the SAG. (c) Picture of twisted SAG sample. Reproduced with permission.[101]

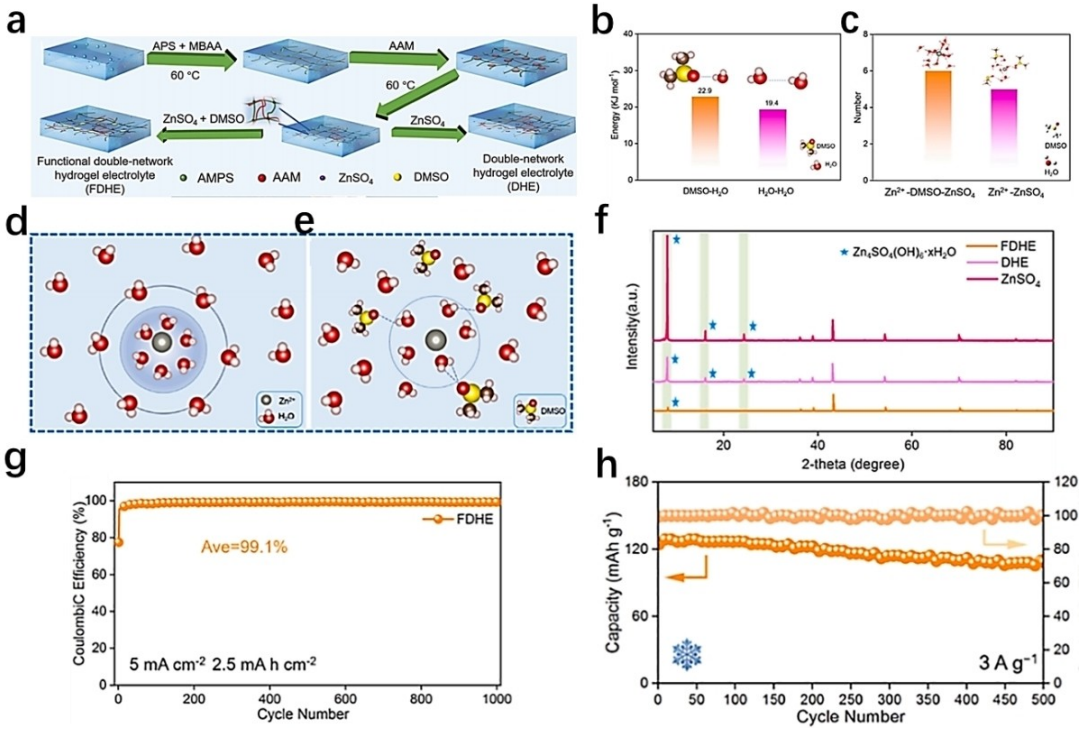

Figure 9. (a) Schematic diagram of the synthesis of PAMPS/PAAM double network hydropolymer. (b) H-bond energies in H_2O–H_2O and H_2O–DMSO calculated by DFT. (c) The water content of Zn^{2+} in the 3.5 Å sheath. Schematic of Zn^{2+} solvation shell of (d) Zn^{2+}–H_2O and (e) Zn^{2+}–H_2O–DMSO systems. (f) XRD patterns of Zn anode after 1000 cycles in different electrolytes. (g) CE measurements of Zn/Cu cells with FDHE at 5 mA cm^{-2}. (h) Cycling stability of Zn/PANI coin cells at 3 A g^{-1} with FDHE electrolytes at −10 °C. Reproduced with permission.[132]

average number of H_2O in the main sheath layer of Zn^{2+} solvation shell decreases from 6 to 5 with the addition of DMSO (Figure 9c). And the schematic diagram of the Zn^{2+} solvation structure also demonstrate that strong hydrogen bonds between DMSO and water molecules are formed, which attracts solvated water molecules, resulting in a decrease in water molecules in the solvation structure of Zn^{2+}(Figure 9d and e). In XRD patterns of Zn anode after 1000 cycles in different electrolytes, there is no obvious signal of by-products on the zinc anode in FDHE (Figure 9f). This confirms that FDHE can effectively reduce side effects. Therefore, when using FDHE electrolyte, the assembled Zn/Cu battery exhibits excellent capacity retention capability at 5 mA cm^{-2} (99.1% after 1000 cycles), and the assembled Zn/PANI battery maintains 85.6% capacity after 500 cycles at −10 °C (Figure 9g and h). Wei et al.[122] proposed a hydropolymer electrolyte (ZS/GL/AN) comprised of polyacrylamide, glycerol, and acetonitrile. The oxygen-containing groups in glycerol display a stronger affinity with water molecules. This can disrupt the hydrogen bonds between water molecules, results in a decrease in the number of active water molecules, and modifies the Zn^{2+} coordination environment. Furthermore, the interaction between Zn^{2+} and oxygen-containing groups preferentially adjusts the shell structure of Zn^{2+} resulting in the uniform deposition of Zn. Consequently, the ZS/GL/AN-assembled Zn//Zn battery demonstrates a cycling time of over 3000 hours and high reversibility (CE of 99.5%). Following 10000 cycles at 5 A g^{-1}, the capacity of the entire battery remains at 88%.

Compared to traditional electrolytes, both high-concentration electrolytes and gel electrolytes have lower free water content, which can inhibit the activity of water molecules, alleviating side reactions.[83,107] However, using high-concentration electrolytes will significantly increase the impedance of batteries and reduce the ion conductivity of batteries due to the adsorption effect between electrolyte molecules.[82,135] Therefore, high-concentration electrolytes are infrequently used in polymer electrolytes. Only a few of studies reported application of the medium concentration electrolytes in polymer electrolytes. For instance, Li et al.[136] developed a new sodium carboxymethyl cellulose (CMC) -medium concentration zinc chloride polymer electrolyte. The electrolyte possesses a notable ionic conductivity of 10.08 mS cm^{-1}. The quasi-solid AZIBs assembled by this electrolyte exhibits considerable energy density (268.2 Wh kg^{-1}) and favorable stability (97.35% after 2800 cycles) (Figure 10a–c).

4. Summary and Outlook

In this review, an overview of the mechanism and influence factors of side reactions in AZIBs is provided. PH and the solvation structure of Zn^{2+} are two main factors that affect side reactions. Due to the solvation effect, solvated water molecules are more likely to participate in HER, corrosion, and the formation of by-products on the interface between the anode and electrolyte. In alkaline electrolytes, zinc metal undergoes

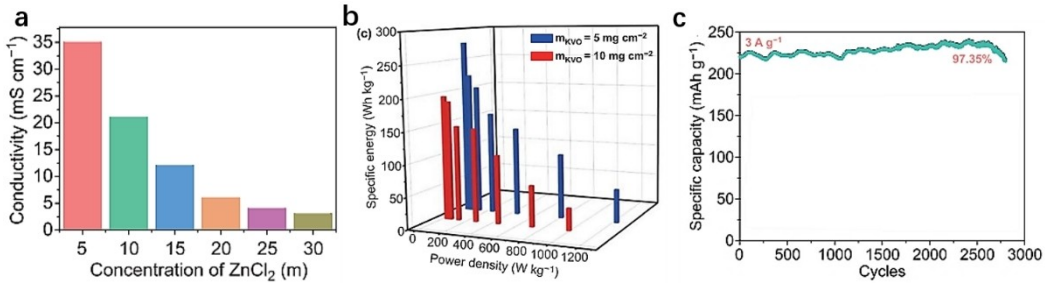

Figure 10. (a) Ionic conductivity values for the $ZnCl_2$ electrolytes with different concentrations. (b) Energy densities and power densities of the cell based on KVO mass. (c) Cyclic performance. Reproduced with permission.[136]

chemical corrosion and generates ZnO by-products. ZnO passivates the surface of the zinc anode, leading to an increase in the internal impedance of batteries. At the same time, ZnO may detach from the zinc anode, leading to irreversibility and capacity degradation of the zinc anode. Taking $ZnSO_4$ electrolyte as an example, in weakly acidic or neutral electrolytes, zinc metal undergoes electrochemical corrosion and generates $Zn_4SO_4(OH)_6 \cdot xH_2O$ by-products. The porous structure of $Zn_4SO_4(OH)_6 \cdot xH_2O$ can not prevent the electrolyte from reaching the surface of the zinc anode. This causes continuous reactions between zinc metal and electrolyte, resulting in a decrease in the CE and cycling performance of batteries. Therefore, modifying the interaction between Zn^{2+} and H_2O molecules, or preventing water molecules from participating in interfacial reactions can effectively alleviate side effects and improve the performance of AZIBs. According to our analysis, optimization strategies for alleviating side reactions are summarized from the perspective of aqueous liquid electrolytes and aqueous polymer electrolytes:

Three optimization strategies are discussed concerning aqueous liquid electrolytes, including optimization of anionic salts, application of additives and regulation of electrolyte concentration. Anionic salts can adjust the solvation structure of Zn^{2+} by substituting water molecules with anions. However, high cost, limited ion conductivity and inadequate performance of some anionic salts in symmetrical cells pose challenges for commercialization. Organic solvent additives and zinc-philic additives are used to alleviate side reactions. These additives can adsorbe on the surface of the zinc anode to form a protective layer, or remove water molecules from the solvation shell of Zn^{2+}. Although additives offer the advantages of low cost, superior safety, and excellent electrochemical performance, they can also increase the energy barrier for Zn^{2+} desolvation and cause electrode polarization, which limits the application of additives. Regulation of electrolyte concentration can inhibit the content and activity of water molecules. High-concentration electrolytes have higher charging and discharging potential windows, higher energy density and lower ionic conductivity. But batteries assembled with high concentration electrolytes are more likely to occur high voltage polarization in low current density situations. This have limited the researches and development of high concentration electrolytes to the laboratory stage.

The special network structure of aqueous polymer electrolytes helps to suppress side reactions. To further optimize polymer electrolytes, two optimization strategies are explored by improving the mechanical strength and water-retention performance of polymer electrolytes, including the modification of the hydrophilic network structure and the electrolyte in the network structure. The hydrophilic network structure is a unique feature of aqueous polymer electrolytes. Strengthen of the hydrophilic network structure can regulate the solvation structure of Zn^{2+} by inhibiting activity water molecules, or indirectly relieve side effects by increasing mechanical strength to suppress zinc dendrites. On the basis of the single network structure composed of typical polymer materials, polymer materials, ionic compounds, and inorganic materials are introduced to optimize the network structure of polymer electrolytes. Hydrophilic groups on polymer materials react with functional groups on synthetic polymer materials to form reversible non-covalent bonds. Materials construct a multi-crosslinked network structure with high water-retention performance through these reversible non covalent bonds. Ionic compounds, including cations and anions, react with functional groups on synthetic polymer materials to form reversible non-covalent bonds, such as ionic and hydrogen bonds, building the physical cross-linking network structure, which gives polymer electrolytes self-healing ability and improves their toughness. Inorganic materials with good conductivity and high mechanical properties are grafted with hydrophilic groups, allowing them to interact with functional groups on synthetic polymer materials to improve the mechanical properties of polymer electrolytes. However, the high cost of some reinforcing materials limits their commercial applications. The optimization of electrolytes in the network structure is mainly achieved by introducing additives. The application of additives is challenging due to the network structure of polymer electrolytes and the complex preparation process for photopolymerization or thermal polymerization. As a result, some additives that lack thermal/optical stability or adsorb on the surface of zinc anodes to exert their effects are unsuitable for application. Some organic solvent additives, which inhibit the activity of water molecules by breaking hydrogen bonds between water molecules, are introduced into polymer electrolytes.

In summary, aqueous polymer electrolytes have significant advantages in solving the problem of side effects because of

their low content of free water molecules. Designing the multi-crosslinked network structure is an important strategy for optimizing polymer electrolytes to alleviate side effects. Enhancing network structures through the introduction of hydrophilic materials stands out as a promising avenue for future development. With their cost-effectiveness and widespread accessibility, natural polymer materials present a plethora of potentially effective hydrophilic candidates. While these materials primarily mitigate side reactions by establishing interactions between functional groups and water molecules, variations in polymer main chains, density of polar groups, and interactions between different functional groups can significantly impact the structure of hydrogen bonding networks, which can affect the performance of electrolytes. At present, the reasons for the differences in hydrogen bonding networks composed of natural materials have not been thoroughly explored. We believe that a deeper comprehension of the mechanisms underlying the formation of these networks in natural materials is imperative to provide robust guidance for material selection and future researches. The polymer electrolytes can be optimized through the modification of hydrophilic network structures or the electrolytes in the network structure. If these two measures are combined, aqueous polymer electrolytes are expected to better mitigate the side reactions. Electrolyte additives are widely used in polymer electrolytes to alleviate side reactions because it can effectively regulate the solvation structure of Zn^{2+}. However, its application in polymer electrolytes, unlike liquid electrolytes, has some new requirements due to the network structure and polymerization process of polymer electrolytes. From the aspect of aqueous electrolyte engineering, the combination of additives and the multi-crosslinked network structure is a more potential development direction in AZIBs.

Acknowledgements

This work is financially supported by the National Natural Science Foundation of China (No. 22075173), the Science and Technology Commission of Shanghai Municipality (No. 19DZ2271100 and 21010501100).

Conflict of Interests

The authors declare no conflict of interest.

Keywords: aqueous electrolyte engineering · polymer electrolyte · side reactions · aqueous zinc ion batteries

[1] B. Bayatsarmadi, Y. Zheng, A. Vasileff, S. Z. Qiao, *Small* **2017**, *13*, 1700191.
[2] D. U. Lee, P. Xu, Z. P. Cano, A. G. Kashkooli, M. G. Park, Z. Chen, *J. Mater. Chem. A* **2016**, *4*, 7107.
[3] K. M. Tan, T. S. Babu, V. K. Ramachandaramurthy, P. Kasinathan, S. G. Solanki, S. K. Raveendran, *J. Energy Storage* **2021**, *39*, 102591.
[4] T. Wu, *ACE* **2023**, *23*, 10–15.
[5] B. Dunn, H. Kamath, J. M. Tarascon, *Science* **2011**, *334*, 928.
[6] M. A. Hannan, M. Lipu, A. Hussain, A. Mohamed, *Renewable Sustainable Energy Rev.* **2017**, *78*, 834.
[7] P. Perumal, S. M. Andersen, A. Nikoloski, S. Basu, M. Mohapatra, *J. Environ. Chem. Eng.* **2021**, *9*, 106455.
[8] Y. Tian, G. Zeng, A. Rutt, T. Shi, H. Kim, J. Wang, J. Koettgen, Y. Sun, B. Ouyang, T. Chen, Z. Lun, Z. Rong, K. Persson, G. Ceder, *Chem. Rev.* **2021**, *121*, 1623.
[9] G. Feng, *ACE* **2023**, *23*, 39.
[10] F. Guo, P. Chen, T. Kang, Y. Wang, L. Chen, *Acta Physico-Chimica Sinica* **2019**, *35*, 1365.
[11] Y. S. Jung, D. Y. Oh, Y. J. Nam, K. H. Park, *Isr. J. Chem.* **2015**, *55*, 472.
[12] Y. Li, S. Wang, J. R. Salvador, J. Wu, B. Liu, W. Yang, J. Yang, W. Zhang, J. Liu, J. Yang, *Chem. Mater.* **2019**, *31*, 2036.
[13] N. Yabuuchi, K. Kubota, M. Dahbi, S. Komaba, *Chem. Rev.* **2014**, *114*, 11636.
[14] C. Arbizzani, G. Lacarbonara, *Pure Appl. Chem.* **2023**, *95*, 1131.
[15] Y. C. Mao, H. Z. Ren, J. C. Zhang, T. Luo, N. N. Liu, B. Wang, S. R. Le, N. Q. Zhang, *Electrochim. Acta* **2021**, *393*, 393.
[16] B. Y. Tang, L. T. Shan, S. Q. Liang, J. Zhou, *Energy Environ. Sci.* **2019**, *12*, 3288.
[17] J. Cao, D. Zhang, X. Zhang, Z. Zeng, J. Qin, Y. Huang, *Energy Environ. Sci.* **2022**, *15*, 499.
[18] X. Zhang, J. P. Hu, N. Fu, W. B. Zhou, B. Liu, Q. Deng, X. W. Wu, *InfoMat* **2022**, *4*, 004.
[19] L. Wang, Z. Cao, P. Zhuang, J. Li, H. Chu, Z. Ye, D. Xu, H. Zhang, J. Shen, M. Ye, *ACS Appl. Mater. Interfaces* **2021**, *13*, 13338.
[20] Z. Wang, J. Diao, J. N. Burrow, K. K. Reimund, N. Katyal, G. Henkelman, C. B. Mullins, *Adv. Funct. Mater.* **2023**, *33*, 2304791.
[21] X. Gong, J. Wang, Y. Shi, Q. Zhang, W. Liu, S. Wang, J. Tian, G. Wang, *Colloids Surf. A* **2023**, *656*, 130255.
[22] Q. Dai, L. Li, B. Hu, Y. Jia, T. Tu, T. K. A. Hoang, M. Zhang, L. Song, *Mater. Today Commun.* **2022**, *31*, 103578.
[23] J. Yang, B. Yin, Y. Sun, H. Pan, W. Sun, B. Jia, S. Zhang, T. Ma, *Nano-Micro Lett.* **2022**, *14*, 42.
[24] Y.-K. Sze, D. E. Irish, *J. Solution Chem.* **1978**, *7*, 417.
[25] C. Zhai, D. Zhao, Y. He, H. Huang, B. Chen, X. Wang, Z. Guo, *Batteries* **2022**, *8*, 153.
[26] X. Lv, W. Wei, H. Wang, B. Huang, Y. Dai, *Appl. Catal. B* **2019**, *264*, 118521.
[27] J. Zhao, J. Zhang, W. Yang, B. Chen, Z. Zhao, H. Qiu, S. Dong, X. Zhou, G. Cui, L. Chen, *Nano Energy* **2019**, *57*, 625.
[28] Z. Li, A. W. Robertson, *Battery Energy* **2022**, *2*, 220029.
[29] Z. Cao, P. Zhuang, X. Zhang, M. Ye, J. Shen, P. M. Ajayan, *Adv. Energy Mater.* **2020**, *10*, 2001599.
[30] S. Huang, S. He, Y. Li, S. Wang, X. Hou, *Chem. Eng. J.* **2023**, *464*, 142607.
[31] Y. Li, J. Yuan, Y. Qiao, H. Xu, Z. Zhang, W. Zhang, G. He, H. Chen, *Dalton Trans.* **2023**, *52*, 11780.
[32] B. Beverskog, I. Puigdomenech, *Corros. Sci.* **1997**, *39*, 107.
[33] Y. Liu, Y. Liu, X. Wu, *Chem. Rec.* **2022**, *22*, e202200088.
[34] Y. Zhang, X. Zheng, N. Wang, W. H. Lai, Y. Liu, S. L. Chou, H. K. Liu, S. X. Dou, Y. X. Wang, *Chem. Sci.* **2022**, *13*, 14246.
[35] N. Guo, W. Huo, X. Dong, Z. Sun, Y. Lu, X. Wu, L. Dai, L. Wang, H. Lin, H. Liu, H. Liang, Z. He, Q. Zhang, *Small Methods* **2022**, *6*, e2200597.
[36] L. Li, S. Jia, M. Cao, Y. Ji, H. Qiu, D. Zhang, *J. Mater. Chem. A* **2023**, *11*, 14568.
[37] S. Xie, Y. Li, X. Li, Y. Zhou, Z. Dang, J. Rong, L. Dong, *Nano-Micro Lett.* **2021**, *14*, 39.
[38] K. Wongrujipairoj, L. Poolnapol, A. Arpornwichanop, S. Suren, S. Kheawhom, *Phys. Status Solidi B* **2017**, *254*, 1600442.
[39] W. Xie, K. Zhu, H. Yang, W. Yang, *Adv. Mater.* **2023**, *36*, 2306154.
[40] Y. Zhou, S. Xie, Y. Li, Z. Zheng, L. Dong, *J. Colloid Interface Sci.* **2023**, *630*, 676.
[41] W. Kao-ian, M. T. Nguyen, T. Yonezawa, R. Pornprasertsuk, J. Qin, S. Siwamogsatham, S. Kheawhom, *Mater. Today* **2021**, *21*, 100738.
[42] J. H. Park, S. H. Park, D. Joung, C. Kim, *Chem. Eng. J.* **2022**, *433*, 433P2.
[43] W. Zhang, C. Zhang, H. Wang, H. Wang, *Chem. Res. Chin. Univ.* **2023**, *39*, 1037–1043. .
[44] P. Jiang, Q. Du, M. Shi, W. Yang, X. Liang, *Small Methods* **2023**, DOI: 10.1002/smtd.202300823e2300823.
[45] C. Liu, X. Xie, B. Lu, J. Zhou, S. Liang, *ACS Energy Lett.* **2021**, *6*, 1015.
[46] W. Y. Chen, S. Guo, L. P. Qin, L. Y. Li, X. X. Cao, J. Zhou, Z. G. Luo, G. Z. Fang, S. Q. Liang, *Adv. Funct. Mater.* **2022**, *32*, 32.
[47] Y. Wang, Z. Wang, F. Yang, S. Liu, S. Zhang, J. Mao, Z. Guo, *Small* **2022**, *18*, e2107033.
[48] M. Hartmann, T. Clark, R. van Eldik, *J. Am. Chem. Soc.* **1997**, *119*, 7843.

[49] N. Zhang, F. Cheng, Y. Liu, Q. Zhao, K. Lei, C. Chen, X. Liu, J. Chen, *J. Am. Chem. Soc.* **2016**, *138*, 12894.
[50] L. Wang, Y. Zhang, H. Hu, H. Y. Shi, Y. Song, D. Guo, X. X. Liu, X. Sun, *ACS Appl. Mater. Interfaces* **2019**, *11*, 42000.
[51] Y. R. Dahal, J. D. Schmit, *Biophys. J.* **2018**, *114*, 76.
[52] K. H. Patel, R. Chockalingam, U. Natarajan, *Mol. Simul.* **2017**, *43*, 691.
[53] Z. Peng, Q. Wei, S. Tan, P. He, W. Luo, Q. An, L. Mai, *Chem. Commun. (Camb.)* **2018**, *54*, 4041.
[54] C. Xu, B. Li, H. Du, F. Kang, *Angew. Chem. Int. Ed.* **2012**, *51*, 933.
[55] Y. Zeng, X. Zhang, Y. Meng, M. Yu, J. Yi, Y. Wu, X. Lu, Y. Tong, *Adv. Mater.* **2017**, *29*, 1700274.
[56] Y. Zhu, J. Hao, Y. Huang, Y. Jiao, *Small Structures* **2023**, *4*, 2200270.
[57] F. Wang, O. Borodin, T. Gao, X. Fan, W. Sun, F. Han, A. Faraone, J. A. Dura, K. Xu, C. Wang, *Nat. Mater.* **2018**, *17*, 543.
[58] C. Sun, R. Miao, J. Li, Y. Sun, Y. Chen, J. Pan, Y. Tang, P. Wan, *ACS Appl. Mater. Interfaces* **2023**, *15*, 20089.
[59] L. Zhang, Z. Liu, G. Wang, J. Feng, Q. Ma, *Nanoscale* **2021**, *13*, 17068.
[60] T. H. Wu, W. S. Lin, *Electrochim. Acta* **2021**, *399*, 139432.
[61] S. Guo, L. Qin, T. Zhang, M. Zhou, J. Zhou, G. Fang, S. Liang, *Energy Storage Mater.* **2021**, *34*, 545.
[62] X. Gong, H. Yang, J. Wang, G. Wang, J. Tian, *ACS Appl. Mater. Interfaces* **2023**, *15*, 4152.
[63] F. Wu, Y. Chen, Y. Chen, R. Yin, Y. Feng, D. Zheng, X. Xu, W. Shi, W. Liu, X. Cao, *Small* **2022**, *18*, e2202363.
[64] H. Lu, X. Zhang, M. Luo, K. Cao, Y. Lu, B. B. Xu, H. Pan, K. Tao, Y. Jiang, *Adv. Funct. Mater.* **2021**, *31*, 2103514.
[65] M. Luo, C. Wang, H. Lu, Y. Lu, B. B. Xu, W. Sun, H. Pan, M. Yan, Y. Jiang, *Energy Storage Mater.* **2021**, *41*, 515.
[66] N. Wang, S. Zhai, Y. Ma, X. Tan, K. Jiang, W. Zhong, W. Zhang, N. Chen, W. Chen, S. Li, G. Han, Z. Li, *Energy Storage Mater.* **2021**, *43*, 585.
[67] J. Hao, L. Yuan, C. Ye, D. Chao, K. Davey, Z. Guo, S. Z. Qiao, *Angew. Chem. Int. Ed. Engl.* **2021**, *60*, 7366.
[68] J. Cao, D. Zhang, R. Chanajaree, Y. Yue, Z. Zeng, X. Zhang, J. Qin, *Adv. Powder Mater.* **2022**, *1*, 100007.
[69] S. J. Zhang, J. Hao, D. Luo, P. F. Zhang, B. Zhang, K. Davey, Z. Lin, S. Z. Qiao, *Adv. Energy Mater.* **2021**, *11*, 2102010.
[70] K. Xie, K. Ren, C. Sun, S. Yang, M. Tong, S. Yang, Z. Liu, Q. Wang, *ACS Appl. Energ. Mater.* **2022**, *5*, 4170.
[71] Q. Gou, H. Luo, Q. Zhang, J. Deng, R. Zhao, O. Odunmbaku, L. Wang, L. Li, Y. Zheng, J. Li, D. Chao, M. Li, *Small* **2023**, *19*, e2207502.
[72] R. Deng, J. Chen, F. Chu, M. Qian, Z. He, A. W. Robertson, J. Maier, F. Wu, *Adv. Mater.* **2023**, *36*, 2311153..
[73] P. Sun, L. Ma, W. Zhou, M. Qiu, Z. Wang, D. Chao, W. Mai, *Angew. Chem. Int. Ed. Engl.* **2021**, *60*, 18247.
[74] C. Huang, X. Zhao, S. Liu, Y. Hao, Q. Tang, A. Hu, Z. Liu, X. Chen, *Adv. Mater.* **2021**, *33*, e2100445.
[75] X. Zhang, J. Chen, H. Cao, X. Huang, Y. Liu, Y. Chen, Y. Huo, D. Lin, Q. Zheng, K. H. Lam, *Small* **2023**, *19*, e2303906.
[76] Y. Quan, M. Yang, M. Chen, W. Zhou, X. Han, J. Chen, B. Liu, S. Shi, P. Zhang, *Chem. Eng. J.* **2023**, *458*, 141392.
[77] L. Chai, J. Pan, X. Zhu, Y. Sun, X. Liu, W. Li, J. Qian, X. Li, X. Sun, *ACS Appl. Mater. Interfaces* **2022**, *14*, 30839.
[78] H. Yan, X. Zhang, Z. Yang, M. Xia, C. Xu, Y. Liu, H. Yu, L. Zhang, J. Shu, *Coord. Chem. Rev.* **2022**, *452*, 214297.
[79] L. Suo, O. Borodin, T. Gao, M. Olguin, J. Ho, X. Fan, C. Luo, C. Wang, K. Xu, *Science* **2015**, *350*, 938.
[80] Z. Yi, G. Chen, F. Hou, L. Wang, J. Liang, *Adv. Energy Mater.* **2021**, *11*, 2170001.
[81] M. Xu, T. Zhu, J. Z. H. Zhang, *J. Phys. Chem. A* **2019**, *123*, 6587.
[82] H. Glatz, E. Tervoort, D. Kundu, *ACS Appl. Mater. Interfaces* **2020**, *12*, 3522.
[83] Y. Yamada, K. Furukawa, K. Sodeyama, K. Kikuchi, M. Yaegashi, Y. Tateyama, A. Yamada, *J. Am. Chem. Soc.* **2014**, *136*, 5039.
[84] Y. Zhu, J. Yin, X. Zheng, A.-H. Emwas, Y. Lei, O. F. Mohammed, Y. Cui, H. N. Alshareef, *Energy Environ. Sci.* **2021**, *14*, 4463.
[85] C. Zhang, J. Holoubek, X. Wu, A. Daniyar, L. Zhu, C. Chen, D. P. Leonard, I. A. Rodriguez-Perez, J. X. Jiang, C. Fang, X. Ji, *Chem. Commun. (Camb.)* **2018**, *54*, 14097.
[86] B. Yang, T. Qin, Y. Du, Y. Zhang, J. Wang, T. Chen, M. Ge, D. Bin, C. Ge, H. Lu, *Chem. Commun. (Camb.)* **2022**, *58*, 1550.
[87] L. Wang, S. Yan, C. D. Quilty, J. Kuang, M. R. Dunkin, S. N. Ehrlich, L. Ma, K. J. Takeuchi, E. S. Takeuchi, A. C. Marschilok, *Adv. Mater. Interfaces* **2021**, *8*, 2002080.
[88] P. Kulkarni, D. Ghosh, R. G. Balakrishna, *Sustain. Energy Fuels* **2021**, *5*, 1619.
[89] Q. Bai, Q. Meng, W. Liu, W. Lin, P. Yi, J. Tang, G. Zhang, P. Cao, J. Yang, *J. Mater. Chem. A* **2023**, *12*, 277–285.
[90] X. Liu, X. Li, X. Yang, J. Lu, X. Zhang, D. Yuan, Y. Zhang, *Chem. Asian J.* **2023**, *18*, e202201280.
[91] Y. Yang, C. Huang, H. Li, Z. Teng, H. Zhang, X. Wei, H. Zhang, L. Wu, C. Zhang, W. Chen, *J. Mater. Chem. C* **2023**, *11*, 9559.
[92] J. Cui, Z. Tao, J. Wu, S. Ma, Y. Yang, J. Zhang, *Small* **2023**, *19*, 2304640.
[93] R. Wang, H. Zhang, Y. Hu, R. Wang, J. Shen, Y. Mao, Q. Wu, B. Wang, *Electrochim. Acta* **2023**, *459*, 142583.
[94] C. Jia, X. Zhang, S. Liang, Y. Fu, W. Liu, J. Chen, X. Liu, L. Zhang, *J. Power Sources* **2022**, *548*, 22232072.
[95] P. Xu, C. Wang, B. Zhao, Y. Zhou, H. Cheng, *J. Power Sources* **2021**, *506*, 107701.1.
[96] Y. Zhang, D. Wu, F. Huang, Y. Cai, Y. Li, H. Ke, P. Lv, Q. Wei, *Adv. Funct. Mater.* **2022**, *32*, 2203204.
[97] T. N. T. Tran, D. Aasen, D. Zhalmuratova, M. Labbe, H. J. Chung, D. G. Ivey, *Batteries & Supercaps* **2020**, *3*, 917.
[98] W. Xu, C. Liu, S. Ren, D. Lee, J. Gwon, J. C. Flake, T. Lei, N. Baisakh, Q. Wu, *J. Mater. Chem. A* **2021**, *9*, 25651.
[99] Y. Huang, J. Liu, J. Wang, M. Hu, F. Mo, G. Liang, C. Zhi, *Angew. Chem. Int. Ed. Engl.* **2018**, *57*, 9810.
[100] D. Liu, Z. Tang, L. Luo, W. Yang, Y. Liu, Z. Shen, X. H. Fan, *ACS Appl. Mater. Interfaces* **2021**, *13*, 36320.
[101] H. Mi, P. Tian, C. Yuan, F. Shi, *Mater. Lett.* **2023**, *330*, 133354.
[102] Y. Yang, W. Li, W. Su, M. Lang, H. Li, F. Zhang, *J. Power Sources* **2023**, *579*, 233313.
[103] Z. F. Liu, C. Y. Zhu, Y. W. Ye, Y. H. Zhang, F. Cheng, H. R. Li, *ACS Appl. Mater. Interfaces* **2022**, *14*, 25962.
[104] H. Zhang, R. Wang, Y. Hu, R. Wang, J. Shen, Y. Mao, Q. Wu, B. Wang, *ACS Appl. Energ. Mater.* **2023**, *6*, 7468.
[105] D. Wang, H. Li, Z. Liu, Z. Tang, G. Liang, F. Mo, Q. Yang, L. Ma, C. Zhi, *Small* **2018**, *14*, e1803978.
[106] W. Xu, C. Liu, Q. Wu, W. Xie, W.-Y. Kim, S.-Y. Lee, J. Gwon, *J. Mater. Chem. A* **2020**, *8*, 18327.
[107] P. Tian, X. Zhong, C. Gu, Z. Wang, F. Shi, *Batteries* **2022**, *8*, 175.
[108] C. Gu, Z. Liu, X. Zhong, Y. Gao, J. Zhao, F. Shi, *Chem. Asian J.* **2023**, *18*, e202300818.
[109] X. Meng, S. Zhou, J. Li, Y. Chen, S. Lin, C. Han, A. Pan, *Adv. Funct. Mater.* **2023**, *34*, 2309350.
[110] J. Lei, J. Xu, N. Ming, L. Dai, C. Zhang, K. Huo, *Ind. Crops Prod.* **2023**, *205*, 117507.
[111] T. Wang, D. He, H. Yao, X. Guo, B. Sun, G. Wang, *Adv. Energy Mater.* **2022**, *12*, 2202568.
[112] C. Jin, J. Nai, O. Sheng, H. Yuan, W. Zhang, X. Tao, X. W. Lou, *Energy Environ. Sci.* **2021**, *14*, 1326.
[113] J. Yang, M. Qiu, M. Zhu, C. Weng, Y. Li, P. Sun, W. Mai, M. Xu, L. Pan, J. Li, *Energy Storage Mater.* **2024**, *67*, 103287.
[114] X. Fu, W. H. Zhong, *Adv. Energy Mater.* **2019**, *9*, 1901774.
[115] F. Tao, L. Qin, Z. Wang, Q. Pan, *ACS Appl. Mater. Interfaces* **2017**, *9*, 15541.
[116] J. Shin, D. S. Choi, H. J. Lee, Y. Jung, J. W. Choi, *Adv. Energy Mater.* **2019**, *9*, 1900083.
[117] T. Zhang, Y. Tang, S. Guo, X. Cao, A. Pan, G. Fang, J. Zhou, S. Liang, *Energy Environ. Sci.* **2020**, *13*, 4625.
[118] S. Huang, L. Hou, T. Li, Y. Jiao, P. Wu, *Adv. Mater.* **2022**, *34*, e2110140.
[119] Y. Shi, R. Wang, S. Bi, M. Yang, L. Liu, Z. Niu, *Adv. Funct. Mater.* **2023**, *33*, 2214546.
[120] H. Li, Y. Liu, Z. Chen, Y. Yang, T. Lv, T. Chen, *J. Colloid Interface Sci.* **2023**, *639*, 408.
[121] E. S. Karaman, S. Mitra, J. Young, *Phys. Chem. Chem. Phys.* **2021**, *23*, 21286.
[122] C. M. Sai Prasanna, S. Austin Suthanthiraraj, *Polym. Compos.* **2019**, *40*, 3402.
[123] S. Prasanna, C. Murali, A. S. Samuel, *J. Appl. Polym. Sci.* **2019**, *136*, 47654.
[124] Y. Li, J. Yuan, Y. Qiao, H. Xu, Z. Zhang, W. Zhang, G. He, H. Chen, *Dalton Trans.* **2023**, *52*, 11780.
[125] Z. Karkar, M. S. E. Houache, S. Niketic, C.-H. Yim, Y. Abu-Lebdeh, *ACS Appl. Energ. Mater.* **2022**, *5*, 14081.
[126] J. Ma, M. Yu, M. Huang, Y. Wu, C. Fu, L. Dong, Z. Zhu, L. Zhang, Z. Zhang, X. Feng, H. Xiang, *Small* **2023**, *20*, 2305649.
[127] Z. H. Wu, A. C. Huang, Y. Tang, Y. P. Yang, Y. C. Liu, Z. P. Li, H. L. Zhou, C. F. Huang, Z. X. Xing, C. M. Shu, J. C. Jiang, *Polymers (Basel).* **2021**, *13*, 1675.

[128] H. Chen, M. Zheng, S. Qian, H. Y. Ling, Z. Wu, X. Liu, C. Yan, S. Zhang, *Carbon Energy* **2021**, *3*, 929.
[129] P. Zhou, K. Sun, S. Ji, Z. Zhao, Y. Fu, J. Xia, S. Wu, Y. Zhu, K. N. Hui, H.-F. Li, *Mater Today Energy* **2023**, *32*, 101248.
[130] K. Kim, T. Kim, G. Song, S. Lee, M. S. Jung, S. Ha, A. R. Ha, K. T. Lee, *Adv. Sci.* **2023**, *10*, 2303308.
[131] I. Dueramae, M. Okhawilai, P. Kasemsiri, H. Uyama, R. Kita, *Sci. Rep.* **2020**, *10*, 12587.
[132] Y. Liu, H. He, A. Gao, J. Ling, F. Yi, J. Hao, Q. Li, D. Shu, *Chem. Eng. J.* **2022**, *446*, 137021.
[133] T. Wei, Y. Ren, Z. Li, X. Zhang, D. Ji, L. Hu, *Chem. Eng. J.* **2022**, *434*, 134646.
[134] R. Wang, M. Yao, S. Huang, J. Tian, Z. Niu, *Sci. China Mater.* **2022**, *65*, 2189.
[135] L. Wang, S. Yan, C. D. Quilty, J. Kuang, M. R. Dunkin, S. N. Ehrlich, L. Ma, K. J. Takeuchi, E. S. Takeuchi, A. C. Marschilok, *Adv. Mater. Interfaces* **2021**, *8*, 2002080.
[136] L. Li, S. Liu, W. Liu, D. Ba, W. Liu, Q. Gui, Y. Chen, Z. Hu, Y. Li, J. Liu, *Nano-Micro Lett.* **2021**, *13*, 34.

Manuscript received: February 10, 2024
Revised manuscript received: March 17, 2024
Accepted manuscript online: March 20, 2024
Version of record online: May 10, 2024